

Review

# Removal of Heavy Metals and Metalloids from Water Using Drinking Water Treatment Residuals as Adsorbents: A Review

Magdalena Wołowiec <sup>1,\*</sup>, Małgorzata Komorowska-Kaufman <sup>2</sup> , Alina Pruss <sup>2</sup> ,  
Grzegorz Rzepa <sup>1</sup> and Tomasz Bajda <sup>1,\*</sup> 

<sup>1</sup> Faculty of Geology, Geophysics and Environmental Protection, AGH University of Science and Technology, al. A. Mickiewicza 30, 30-059 Krakow, Poland

<sup>2</sup> Institute of Environmental Engineering, Poznan University of Technology, Faculty of Civil and Environmental Engineering, ul. Berdychowo 4, 60-965 Poznań, Poland

\* Correspondence: wolowiec@agh.edu.pl (M.W.); bajda@agh.edu.pl (T.B.); Tel.: +48-500-032-026 (M.W.); +48-12-617-52-32 (T.B.)

Received: 18 June 2019; Accepted: 13 August 2019; Published: 14 August 2019



**Abstract:** Heavy metal contamination is one of the most important environmental issues. Therefore, appropriate steps need to be taken to reduce heavy metals and metalloids in water to acceptable levels. Several treatment methods have been developed recently to adsorb these pollutants. This paper reviews the ability of residuals generated as a by-product from the water treatment plants to adsorb heavy metals and metalloids from water. Water treatment residuals have great sorption capacities due to their large specific surface area and chemical composition. Sorption capacity is also affected by sorption conditions. A survey of the literature shows that water treatment residuals may be a suitable material for developing an efficient adsorbent for the removal of heavy metals and metalloids from water.

**Keywords:** adsorption; arsenic; pollutants; water treatment sludges

## 1. Introduction

Heavy metals are a group of trace elements that include metals and metalloids, such as arsenic, cadmium, chromium, cobalt, copper, iron, lead, manganese, mercury, nickel, tin, and zinc. They have a relatively high density of over  $4 \times 10^6$  mg/L. The metal ions are known to contaminate the soil, atmosphere, and water systems and are poisonous even in very low concentrations [1]. There are two main sources of heavy metals in water—natural and anthropogenic. Natural sources comprise volcanic activities, soil erosion, activities of living organisms, and weathering of rocks and minerals, whereas anthropogenic sources include landfills, fuel combustion, street run-offs, sewage, agricultural activities, mining, and industrial pollutants, such as textile dyes [2]. Heavy metals are classified as toxic and carcinogenic, they are capable of accumulating in tissues and cause diseases and disorders (Table 1).

**Table 1.** Comparison of selected heavy metals, their anthropogenic sources, provisional maximum tolerable daily intake (PMTDI) according to WHO, and symptoms and diseases.

Heavy Metal	Anthropogenic Sources	PMTDI (mg/L)	Symptoms and Diseases	References
As	Pesticides, biosolids, disposal of industrial wastes, mining activities, feed additives, insecticides, ceramics, veterinary medicine, metallurgy, herbicides, electronic components, electrical generation, tanning, and textile	0.01	Arsenicosis, cancers of the bladder, skin, lungs, and kidneys	[3,4]
Cd	Petroleum refining, electroplating and alloying industry, nickel–cadmium batteries, coal combustion, plastic stabilizers	0.003	Emphysema, hypertension, nephropathy, diabetes mellitus, skeletal malformation	[5]
Cr	Pigments, chemicals, electroplating, coating operations, wood treatment, data storage, textiles and leather tanning, metallurgy	0.05	Allergic reactions, skin rash, nose irritations, nosebleed, ulcer, weakened the immune system, genetic material alteration, kidney and liver damage, cancer	[6,7]
Co	Preparation of semiconductors, nuclear medicine, enamel and painting on glass, grinding wheels, porcelain, hydrometers, electroplating, aerospace materials, Li-ion batteries	0.002	Paralysis, diarrhea, lung irritation, bone defects, low blood pressure, genetic changes in cells	[8]
Cu	Mining operations, chemical, and pharmaceutical equipment, kitchenware, paper manufacturing	1.5	Menkes, Wilson, Alzheimer’s, Parkinson’s diseases, damages for eye and liver, vomiting, cramps, convulsions	[9]
Fe	Iron and steel industries, mining, metal corrosion	No guideline	Hemochromatosis, eyes disorder, cancer, and heart diseases	[10]
Pb	Fuels, manufacturing of electronic products, metal processing, painting pigments, electroplating, leather tanning and mining	0.01	Reproductive system damage, central nervous system damage, liver and kidneys diseases	[11]
Hg	Mining operations, tanneries, dental filling, solders, Hg vapor lamps, metal plating facilities, amalgamation, catalysts, pharmaceuticals, rectifiers, fungicides	0.001	Kidneys, lungs and eyes diseases, skin dermatitis, nervous system dysfunction	[12]
Mn	Corrosion of iron pipes, production of manganese steels, ferromanganese alloys	0.5	Lethargy, tremors, psychological disturbances, respiratory infections	[13]
Ni	Nickel steel, non-ferrous alloys, superalloys, electroplating, alnico magnets, coinage, microphone capsules, rechargeable batteries, plating on plumbing fixtures, catalysts, dental and surgical prostheses	0.02	Anemia, diarrhea, encephalopathy, hepatitis, lung and kidney damage, gastrointestinal distress, pulmonary fibrosis, renal edema, skin dermatitis, central nervous system dysfunction.	[14,15]
Zn	Batteries, pigments, Zn alloys, rubber industry, chemical industry, paints, cans, anti-corrosion coating	3	Depression, lethargy, respiratory incapacitation, appetite loss, diarrhea, headaches	[16]

Contamination of aquatic systems is a serious environmental issue and therefore the development of an efficient and suitable technology to remove heavy metals from aqueous solutions is necessary. Several methods have been used to remove heavy metals from contaminated water. They include chemical precipitation [17,18], ion exchange [19,20], adsorption [21,22], membrane filtration [23,24], reverse osmosis [25,26], solvent extraction [27], and electrochemical treatment [28,29]. Many of these methods suffer from high capital and operational costs. Adsorption seems to be one of the best-suited methods, due to its high efficiency, low-cost, and ease of operation. Various adsorbents, such as carbon foam [30], activated carbon [31], zeolite [32], clay minerals [33,34], organic polymers [35], and biochar [36], and many waste materials, such as fly ash [37], reused sanding wastes [38], biomass [39], and water treatment residuals (WTRs) [40,41], have been used for the removal of heavy metals by adsorption. The most effective heavy metal adsorbents, especially for arsenic, are adsorbents based on metal oxides (Fe, Al, Mn oxides), such as WTRs, bog iron ores [42], ferrihydrite [43], goethite [44], layered double hydroxide (LDH) [45], Sn/Ti-Mn binary metal oxides [46,47], Al/Fe oxide-oxyhydroxide composite powders [48], and red mud [49].

Using waste products as adsorbents provides many benefits. It decreases the cost of removing metals from water, as well as being conducive to decreasing amounts of residuals which are accumulated in the environment.

WTRs, sometimes referred to as water treatment sludge or waterworks sludge, are by-products generated by drinking water treatment plants. Each year, several million tons of WTRs are produced [50–54]. Their disposal is problematic and expensive due to environmental restrictions and has provided the impetus for research into their reuse [55]. Proper handling of huge amounts of WTRs in an economical and environmentally friendly manner is, therefore, a very significant issue. The feasibility of managing WTRs is determined by their chemical composition and properties, which are diversified due to the wide variation in the type and chemical composition of raw water, geology, and hydrogeology of the intake area, as well as water treatment technology.

In recent years, an increasing number of studies have addressed the use of WTRs to remove pollutants from aqueous solutions. Most of the research is focused on the precipitation of phosphorous from wastewater [56,57]. Researchers indicate that WTRs are characterized by good sorption properties [51,58–61]. The aim of the present research was to present a review of the studies that have evaluated WTRs as heavy metals sorbents.

## 2. Materials and Methods

### 2.1. Materials

In this review, the authors provide collected researches concerning the sorption capacity for heavy metals and metalloids of post-coagulation residuals of surface water treatments (SWTRs) and residuals of deironing and demanganization processes of groundwater treatments (GWTRs) as there is no similar review. The comparison of research is crucial due to the necessity to find the most effective methods of using sludges as sorbents. The authors reviewed publications describing the characteristics and sorption properties of SWTRs or GWTRs. They focused on the research papers reported within 10 years as there is also an increase in interest in the use of sludge from water treatment. The methodology and parameters of sorption and results as a function of time, pH, sorbent dose, initial concentration, and temperature were presented. Additionally, the parameters at which the sorption was most effective were indicated. The authors compared the sorption values of individual heavy metals and metalloids on SWTRs and GWTRs. They also described the part of their research on the sorption capacity of heavy metals and metalloids on GWTRs.

### 2.2. Authors' Research

GWTRs generated as a by-product of the deironing process of underground water were used in the experiments. The sample was collected from a water treatment station in Wielkopolska

Voivodship, Poland. Samples of GWTRs were dried and ground in a mortar and sieved using a 1 mm sieve to remove large particles. The phase composition was determined by X-ray powder diffraction (RIGAKU SmartLab Diffractometer, RIGAKU, Tokyo, Japan). To observe the surface and performing microanalyses the electron microscopy using a variable pressure field emission scanning electron microscope (FEI Quanta 200, Graz, Austria) was used. The  $S_{\text{BET}}$  was determined from  $\text{N}_2$  gas adsorption/desorption isotherms at 77 K after outgassing for 12 h at 373 K using an ASAP 2020 apparatus (Micrometrics, Norcross, GA, USA).

Static sorption experiments were carried at a Liquid to Solid (L/S) ratio equal to 1:20 (5 mL solution + 100 mg sample). The reaction time was 24 h. The pH of the stock solution was not regulated. The experiments were conducted at room temperature. The influence of Cd(II), Pb(II), Zn(II), Cu(II), Cr(III), Cr(VI) and As(V) concentration (0.1, 1, 10, and 100 mM/L) on the sorption capacity was investigated. The source of ions was analytical grade reagents:  $\text{Cd}(\text{NO}_3)_2 \cdot 4\text{H}_2\text{O}$ ;  $\text{Pb}(\text{NO}_3)_2$ ;  $\text{Zn}(\text{NO}_3)_2 \cdot 6\text{H}_2\text{O}$ ;  $\text{CuN}_2\text{O}_6 \cdot 3\text{H}_2\text{O}$ ;  $\text{K}_2\text{Cr}_2\text{O}_7$ ;  $\text{CrN}_3\text{O}_9 \cdot 9\text{H}_2\text{O}$ ;  $\text{Na}_2\text{HAsO}_4 \cdot 7\text{H}_2\text{O}$ , respectively. The concentrations of selected heavy metals and metalloids in an equilibrium solution was analyzed by atomic absorption spectroscopy (AAS) (SavantAA GBC Scientific Equipment, Braeside, Australia) and UV-Vis spectrophotometry (Hitachi U-1800, Berkshire, UK).

### 3. Material Characterization

In this review, some SWTRs and GWTRs were compared. The chemical composition and properties of the WTRs are diversified and depend on their origin (surface or groundwater) and chemical composition of the treated water and/or methods and materials used for water treatment.

#### 3.1. Post-Coagulation Residuals

Usually, surface water carries suspended and colloidal solids, organic compounds, and other contaminants. Water treatment includes processes, such as coagulation, flocculation, sedimentation, and filtration, for the removal of color, turbidity, and other contaminants. The most common coagulants are iron salts (e.g.,  $\text{FeCl}_3 \cdot 6\text{H}_2\text{O}$ ;  $\text{FeCl}_2$ ;  $\text{FeSO}_4 \cdot 7\text{H}_2\text{O}$ ;  $\text{Fe}_2(\text{SO}_4)_3 \cdot 7\text{H}_2\text{O}$ ) and aluminum salts (e.g.,  $\text{Al}_2(\text{SO}_4)_3 \cdot 18\text{H}_2\text{O}$ ;  $\text{AlCl}_3$ ;  $\text{Na}_2\text{Al}_2\text{O}_4$ ) [62]. Aluminum salts are preferred for water treatment. They hydrolyze in water to aluminum hydroxide and then the colloidal and suspended contaminants are removed by charge neutralization, sweep floc mechanism, and adsorption onto hydroxide precipitates [63]. Sludges generated from surface water treatments are called post-coagulation residuals and their composition depends on the coagulant used—iron (Fe-SWTRs) or aluminum (Al-SWTRs) [59]. Al-SWTRs are composed mainly of aluminum oxide, whose content in the sludge varies in the range 14.5–46.0% [64–66]. A major component of Fe-SWTRs is iron oxide varying in weight fraction from 15.5% to 26% [55]. Significant amounts of  $\text{SiO}_2$  (26.2–41.8%) are also present in both types of SWTRs [55,64]. The content of organic substances can even reach 25% [67].

The elemental composition of SWTRs is shown in Table 2. The main elements of SWTRs generated during surface water treatment are Al and (some) Fe, which are components of coagulants [41]. With an increase in the coagulant dosage, the amounts of Al and Fe also increase. A high organic carbon (C) content comes from organic compounds removed from the water or from activated carbon used for treatment [4,68]. Significant concentrations of Ca, Mn, and Mg are also present as are heavy metals in low concentrations. For example, in the case of Al-SWTRs, concentrations of Cu, Zn, Cr, Cd, Pb, and As are 0.005–0.007, 0.009–0.011, 0.008–0.039, 0.001–0.028, 0.005–0.008, and 0.013–0.037 mg/L, respectively [69]. Using WTRs as adsorbents, the materials should be considered as non-toxic wastes. As previous research shows, the release of metals from WTRs is negligible and therefore, they are non-toxic wastes [59,70]. Zhou and Haynes [68,69] also conducted leaching test. resulting in very low Cu, Zn, Cr, Cd, Pb, and As concentration in the leachate, below the respective USEPA (United States Environmental Protection Agency) regulatory guidelines for toxic wastes [71].

**Table 2.** The concentration of selected elements in the post-coagulation water treatment residuals. (PAC—polyaluminum chloride, AC—activated carbon).

Water Origin	Water Treatment Process	Chemical Composition (mg/g)						References
		Fe	Al	Ca	Mn	Mg	C	
Surface water	Fe and Al coagulation	71.2	62.7	18.9	2.9	2.4	-	[41]
	Al coagulation	17.8	74.7	15.7	0.8	4.5	-	[72]
	Al coagulation	23.9	122.0	0.4	-	0.2	103.0	[69]
	Al coagulation + AC	17.2	73.5	0.4	-	1.8	346.0	
	Al coagulation	4.0	95.3	-	-	-	243.0	[4]
	Fe coagulation	161.0	1.2	-	-	-	155.0	
	Al coagulation (PAC)	17.5	63.6	-	1.2	1.2	-	[73]
	Al coagulation + AC (PAC)	11.5	53.3	-	1.4	2.3	-	
Groundwater	Aeration + pre-chlorination + Al coagulation + filtration	26.0–90.0	105.0–144.0	3.2–3.6	0.03–1.1	0.2–2.3	-	[57]

Scanning electron microscopy (SEM) analysis shows that Fe- and Al-SWTRs are heterogeneously mixed particles with irregular shapes and a variable pore diameter (0.6–4.3 nm), which prospectively guarantee a highly reactive surface that favors the sorption [41,52]. X-ray diffraction (XRD) patterns show that post-coagulation residuals are amorphous and poorly ordered. However, some Fe-SWTR samples have peaks attributed to small amounts of crystalline Fe-(hydr)oxides [4]. Analysis similarly shows that Al-SWTRs contain quartz, calcite, feldspar, and sometimes illite/smectite and kaolinite as well [72].

### 3.2. Groundwater Treatment Residuals

In most cases, groundwater is treated to remove iron and manganese. This is achieved by aeration and filtration [54]. The soluble Fe(II) form is oxidized to the insoluble Fe(III) form and the flocs are captured on the filter bed [67]. Further oxidation of Fe and Mn takes place in the filter bed, enhancing filter effectiveness. As long as there are no other pollutants in the water, no additional chemicals need to be used in this process [53,74–76]. The filters are periodically backwashed, and the contaminants retained in the filter bed during the water purification process are washed away and collected in a clarifier. These pollutants settle and form sediments in the clarifier and the resulting sludge is known as the residual from deironing and demanganization of ground or infiltration water (Fe/Mn-GWTRs) [74–77]. The main components of Fe/Mn-GWTRs are iron and manganese compounds, especially oxides [54,67]. Fe/Mn-GWTRs contain iron oxides (24.3%), manganese oxides (5.35%), organic carbon (5.3%), and inorganic carbon (0.73%) [40].

Fe, at a concentration of 300 mg/g, is the main component of WTRs generated by groundwater treatment processes [57]. A significant amount of Ca is also present. The concentration of these metal ions appears to be influenced by the quality of raw water. The WTRs also contain low concentrations of heavy metals [40].

A typical SEM image and XRD pattern of WTRs are given in Figure 1. The samples of GWTRs reveal a typical microcrystalline-organogenic microstructure, with small carbonate crystals embedded within substantial cryptocrystalline aggregated iron oxyhydroxides. The particles have irregular surfaces with edges. The residuals are poorly crystalline, just like Al/Fe-GWTRs; however, the two-line ferrihydrite can be noted. The low-intensity XRD peaks are indicative of quartz and calcite. All GWTRs presented in this research [40,53,61] show a similar phase composition, indicating that sludge are rather amorphous material; the only crystalline mineral that was found was quartz [40].

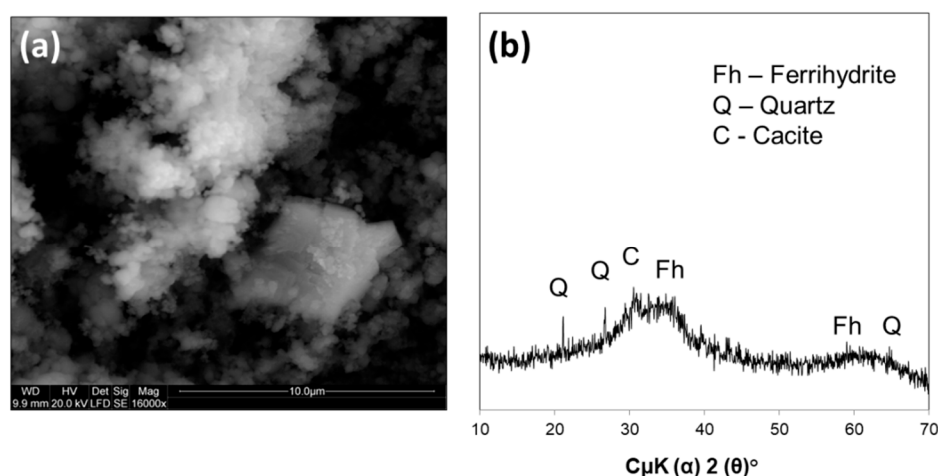


**Figure 1.** Water treatment residuals (a) SEM image; (b) X-ray diffraction pattern (author’s materials).

### 3.3. Physicochemical Properties and Textural Parameters

Some properties of the residuals, such as textural parameters and chemical composition, influence the sorption capability.

The residuals exhibit a wide range of specific surface area values, which depend on different factors. As can be seen, typical surface water treatment residuals display relatively high specific surface areas in the range of 80 to 100 m<sup>2</sup>/g (Table 3), when only Al and Fe salts are added. An addition of activated carbon increases the specific surface of the sludge. The particle size is extremely significant for the specific surface area. Caporale et al. [4] noted that decreasing WTRs' particle size in the range 1000–590 µm to below 125 µm increased the surface area of the sludge by almost 80% in the case of Fe-WTRs. Residuals from groundwater treatment displayed similar values of surface area: 120–170 m<sup>2</sup>/g.

**Table 3.** Comparison of some physical properties of WTRs (water treatment residuals). (PAC—polyaluminum chloride).

Water Origin	Water Treatment Process	Particle Size	Specific Surface Area (m <sup>2</sup> /g)	pH	References
Surface water	Al & Fe coagulation	<165 µm	81	7.6	[41]
	Al coagulation	<125 µm	97	6.8	[69]
	Al coagulation + AC	<125 µm	290	6.5	
	Al coagulation	<125 µm	435	5.5	[4]
	Fe coagulation	<125 µm	217	6.1	
	Al coagulation (PAC)	<1 mm	50	5.6	
		Al coagulation + AC (PAC)	<1 mm	413	5.6
Groundwater	No reagents	<1 mm	120	-	[40]
	No reagents	<60 µm	152	7.0	[61]
	No reagents	<1 mm	170	-	This study

The structure and chemical composition of, especially, the metal oxides in WTRs, because of their heterogeneous nature with irregular shapes and a variable pore diameter, provide acceptable sorption properties. A key factor is that the residuals are dominated by amorphous oxides, which increase sorption capabilities in comparison to materials composed of more crystalline forms [78].

## 4. Results

### 4.1. Adsorption Capacity of Post-Coagulation Residuals

Ippolito et al. [72] showed that Al-SWTRs were a good selenium adsorbent. In 100 mL of 0.05 M NaCl solution, 2.5 g SWTRs was mixed with an appropriate amount of Na<sub>2</sub>SeO<sub>4</sub> or Na<sub>2</sub>SeO<sub>3</sub> to provide an Se(IV) and Se(VI) concentration of 60 mg/L. They stated that pH did not affect the adsorption of selenate and selenite. Al-SWTRs adsorbed Se(VI) and Se(IV) in amounts of 1.4 to 2.1 mg/g and 1.4 to 1.95 mg/g, respectively. Se(VI) adsorbed on the Al-SWTRs occurred as outer sphere complexes, while Se(IV) created inner-sphere complexation. The absence of inner-sphere complexation in case of Se(VI) implies that iron hydroxide impurities in Al-SWTRs have limited impact on Se(VI). In the 5–8 pH range, Se(IV) was reduced to Se(0). The adsorption was governed by the mixture of clay minerals and amorphous aluminum oxides.

Siswoyo et al. [73] showed that SWTRs are a good cadmium(II) adsorbent. Different doses of the adsorbent were added to 50 mL of Cd(II) solution at different concentrations. The effect of pH and time was evaluated. The maximum sorption capacities were 5.3 and 9.2 mg Cd/g, according to the Langmuir adsorption model. The SWTRs were strongly dependent on the pH of the solution. The removal efficiency of Cd(II) increased with the pH of the solution due to a decrease in H<sup>+</sup> on the surface, which results in less repulsion with the metal ions [79]. The favorable pH was in the range of 6.0 to 8.0. The amounts of adsorbed Cd(II) increased with an increase in the adsorbent dosage due to the greater accessibility of the surface area or binding sites [80,81]. The Cd(II) adsorption capacity

increased rapidly for 30 min and then become constant until 24 h of shaking. The feasible mechanism of cadmium ion adsorption on SWTRs is the ion exchange model [82].

The capability of SWTRs for removing mercury was reported by Hovsepian and Bonzongo [59]. Commercial  $\text{Hg}(\text{NO}_3)_2$  were used to prepare  $\text{Hg}(\text{II})$  solutions with different concentrations for batch sorption experiments. The solutions were kept in contact with dry Al-SWTRs in a 3:5 ratio. The maximum sorption capacity achieved was 79 mg Hg/g according to the Langmuir equation. Sorption isotherms indicated a strong affinity of  $\text{Hg}(\text{II})$  for Al-SWTRs. The highest  $\text{Hg}(\text{II})$  removal efficiency was at pH 3.0 and the lowest at 5.0. The equilibrium was achieved in about 32 h. The best-fit equation for sorption kinetic data was a pseudo-first-order model, while use of the Weber–Morris and Bangham models indicated that the intraparticle diffusion might be the rate-limiting step for the  $\text{Hg}(\text{II})$  immobilization on Al-SWTRs. The authors noted that further research concerning sorption mechanisms and the long-term stability of the created Hg with Al-SWTRs complexes is needed.

Though several studies have demonstrated the ability of SWTRs to efficiently sorb metal ions from aqueous solutions, the mechanisms of metal sorption are still not fully understood. Quiñones et al. [52] carried out research on the sorption of mercury cations by Al-SWTRs and focused on the sorption mechanisms. They used a flooding technique followed by wet and dry cycles to prepare Hg-spiked Al-SWTR samples. A known amount of Al-SWTRs is brought into contact with an  $\text{HgCl}_2$  solution at a 1:4 ratio. Three different types of Al-SWTRs samples were prepared. Different methods were used to determine the binding mechanisms of  $\text{Hg}(\text{II})$  and Al-SWTRs. A significant fraction of the added Hg was found to be locked in the residual fraction and was not mobile under natural environmental conditions. The organic  $\text{Hg}(\text{II})$  fraction of Al-SWTRs, after the spiking and aging, was found to be prone to methylation by bacteria. However, there was significant immobilization of  $\text{Hg}(\text{II})$  by Al-SWTRs due to its binding to oxygen donor atoms of mineral ligands. Quiñones et al. [52] have also suggested that the use of additional methods, such as XANES (X-ray Absorption Near Edge Structure) and EXAFS (Extended X-ray Absorption Fine Structure), is necessary to explain the different bonds between  $\text{Hg}(\text{II})$  and electron donors more precisely.

Jiao et al. [41] reported SWTRs as effective cobalt(II) adsorbents. Batch adsorption experiments were carried out by agitating 0.5 g of SWTRs with 30 mL aqueous solution containing 0 to 800 mg/L of  $\text{Co}(\text{II})$  on a shake table at a constant temperature of 25 °C. The sorption of  $\text{Co}(\text{II})$  followed pseudo-second-order kinetics. Moreover, 90% of the equilibrium sorption capacity has been reached within the first 12 h. The adsorption of  $\text{Co}(\text{II})$  was a two-step process [83]- quick adsorption of  $\text{Co}(\text{II})$  on the external surface and possible slow intraparticle diffusion in the interior of the SWTR particles. The sorption isotherm was well-fitted by the Langmuir model. The maximal adsorption capacity reached 17.307 mg/g.  $\text{Co}(\text{II})$  removal was enhanced with increasing pH; this trend might be explained due to the changes in the surface charge characteristics of the SWTRs with pH [84]. Adsorption is a spontaneous endothermic process. During desorption of  $\text{Co}(\text{II})$ , only minimal amount of compound was desorbed, and the process was strongly dependent on pH. Decreasing pH values might enhance  $\text{Co}(\text{II})$  desorption. According to the FTIR analysis, the possible sorption mechanism is the formation of inner or outer sphere complexes between adsorbed  $\text{Co}(\text{II})$  and the surface hydroxyl groups existing on the surface of the SWTRs.

Zhou and Haynes [69] examined other Al-SWTRs for  $\text{Pb}(\text{II})$ ,  $\text{Cr}(\text{III})$ , and  $\text{Cr}(\text{VI})$  removal. Metal solutions of  $\text{Pb}(\text{NO}_3)_2$ ,  $\text{Cr}(\text{NO}_3)_3$ , and  $\text{Na}_2\text{CrO}_4$ , with the desired metal concentration, were prepared in 0.01 M  $\text{NaNO}_3$  solution. A measured amount of sludge was weighed into 50 mL centrifuge tubes and 10 mL of 0.01 M  $\text{NaNO}_3$  was added. Adsorption capacity was highly dependent on the initial metal ion concentration, initial pH, and dosage. Adsorption of all compounds increased with an increasing equilibrium concentration of the adsorbate.  $\text{Cr}(\text{III})$  and  $\text{Pb}(\text{II})$  were preferably adsorbed at pH 6.0 to 9.0, which is typical for heavy metal cations [85], whereas  $\text{Cr}(\text{VI})$  was adsorbed most effectively at pH 2.0–4.0. It was found that equilibrium was reached in 120 min and 90% of maximum sorption had occurred. The higher the adsorbent dose was, the higher the amount of adsorbed metal ions due to an increase of the surface area and number of adsorption sites. Adsorption increased with an increasing

temperature between 20 and 50 °C, suggesting that sorption is an endothermic process. The sorption isotherm was well fitted to the Freundlich and Langmuir equations. The maximum adsorption capacities of Pb(II), Cr(III), and Cr(V) were 53.87–62.16 mg/g, 19.24–26.52 mg/g, and 10.92–11.44 mg/g, respectively. Kinetic data was correlated to a pseudo-second-order kinetic model for Cr(III) and Pb(II), implying that chemisorption was the rate-limiting step to sorption [86].

Makris et al. [87] were one of the first groups to deal with arsenic sorption onto Fe-SWTRs and Al-SWTRs. As sorption capacities of the WTRs were determined in batch equilibrium studies. Stock standard solutions were prepared in 0.01 M KCl. The pH was adjusted to 6.0. An initial screening study was performed to evaluate the effectiveness of both SWTRs in removing As from the solution at a fixed solid solution ratio (1:10). Detailed experiments were conducted to determine the effect of the solid-solution ratio and time; pH was not controlled. Al-SWTRs sorbed greater amounts of As(V) than Fe-SWTRs (1.88–15 mg/g); however, As(III) was more preferably removed by Fe-SWTRs (7.5–15 mg/g). Al-SWTRs had greater sorption capabilities due to the higher specific surface area. Additional spectroscopic analysis should be conducted to explain the differences in As(III) and As(V) sorption. The sorption isotherm was well fitted to the Freundlich equations. Sorption of As(III) and As(V) was a biphasic process. The beginning of the sorption was rapid; within the first hour, 98% of the compound was removed, followed by a slower sorption rate. Kinetic data was correlated to a pseudo-second-order kinetic model.

Zhou and Haynes [68] again examined Al-SWTRs for As(III), As(V), Se(IV), and Se(VI) removal. Metal solutions of NaAsO<sub>2</sub>, Na<sub>2</sub>HAsO<sub>4</sub>, Na<sub>2</sub>SeO<sub>3</sub>, and Na<sub>2</sub>SeO<sub>4</sub> with the desired metal concentration were prepared in 0.01 M NaNO<sub>3</sub>. Materials and methodology were identical to those presented by Zhou and Haynes [69]. Adsorption was strongly dependent on the pH. The adsorption decrease was rapid above pH 4.0 for Se(VI), above pH 5.0 for Se(IV), and above pH 6.0 for As(V). Adsorption of As(III) increased with increasing pH up to pH 9.0, then decreased. The sorption isotherm was well fitted to the Freundlich and Langmuir equations. The As(III), As(V), Se(IV), and Se(VI) maximum adsorption capacities were 18.73, 20.98, 22.11, and 11.05 mg/g, respectively. Kinetic data were correlated to a pseudo-second-order kinetic model. The adsorption was rapid; equilibrium occurred after 120 min. Chemisorption was the rate-limiting step for adsorption. The study demonstrated that the metals were strongly bonded to the sludge surface and so they could not be easily leached from the material.

Caporale et al. [4] reported another As-adsorbing Al-SWTRs and Fe-SWTRs. The authors investigated the effect of the particle size of adsorbents on sorption. Four samples of Al-SWTRs and Fe-SWTRs with different particle sizes were obtained. The solution volume was adjusted to 20 mL with 10 mmol/L KCl and the initial SWTRs-solution ratio was fixed at 5 g/L. The effects of pH (3.0–9.0) was investigated. The equilibrium data was well fitted to the Langmuir equation. As(III) was more preferably sorbed than As(V) by Fe-WTRs, whereas As(V) was more willingly sorbed than As(III) by Al-SWTRs. Because of their higher surface area, the Al-SWTRs were more effective sorbents. More efficient removal of As was achieved by decreasing the SWTRs' particle size. The specific surface area of the smallest particles of Fe-SWTRs and Al-SWTRs increased by 137 and 123 m<sup>2</sup>/g, respectively. The maximum adsorption capacities of Fe-SWTRs and Al-SWTRs with particle sizes <125 μm were 11.21 and 40.24 mg/g for As(III) and 9.19 and 49.98 mg/g for As(V). However, the effect of the particle size was more evident in the case of Fe-SWTRs than Al-SWTRs. It might be caused by a large increase in the surface area of SWTRs containing Fe corresponding to the decrease in particle size. The highest sorption of As(III) and As(V) by Al-SWTRs was noted at pH 6.0 to 7.0, whereas the adsorption capacity of Fe-SWTRs seemed to be independent of pH.

Other As(V) adsorbing SWTRs were reported by Elkhatib et al. [3]. They synthesized WTRs on a nanoscale (nSWTRs), with particle sizes <100 nm. Adsorption studies were conducted at pH 7.2 and the effect of pH, time, dosage of nSWTRs, and the initial concentration was determined. As(V) adsorption was highest at pH 3 (88%) and the least at pH 11 (14.9%), due to the increase in the coulomb repulsive force between the surface of SWTRs and As(V) as the solution pH increases [70]. The equilibrium data was well-fitted to the Langmuir and Temkin models. Adsorption of As(V) was

biphasic, consisting of a rapid sorption followed by much slower sorption phase. The maximum As(V) sorption capacity reached was 50 mg/g. nSWTRs achieved a higher maximum sorption capacity than  $\mu$ WTRs (<51  $\mu$ m) and mWTRs (2 mm). A possible mechanism for As(V) sorption was the formation of bidentate (adsorption of arsenate ions onto iron hydroxides) and monodentate (adsorption of As(V) onto aluminum hydroxides) surface complexes. The power function model best described As(V) adsorption on nSWTRs. The results of the desorption process point to the stability of As-SWTRs surface complexes.

#### 4.2. Adsorption Capacity of Groundwater Treatment Residual

Wu et al. [61] reported the possible usage of Fe-based backwashed sludge for arsenite removal from water. In the sorption study, 0.06 g of GWTRs was added to 100 mL of As(III) solution with different initial concentrations. The maximum adsorption of As(III) reached was 59.7 mg/g, according to the Langmuir model. The As(III) removal efficiency was strongly dependent on the solution pH, with the best results obtained for pH 8.0. The subsequent increase of pH led to decrease of sorption effectiveness due. It could be assigned to the electrical repulsion between GWTRs and As(III) anions [88]. Higher adsorbent dosages resulted in higher As(III) removal efficiency. The removal of As(III) increased rapidly in the first 1 h, however, equilibrium adsorption was reached after 18 h. The kinetic data correlated with both the Elovich model and the power model. Adsorption was an endothermic process, which is in line with other researches [41,69]. The removal of As(III) by GWTRs was mainly controlled by adhesion and ligand exchange between the As species and sulfate. Desorption results show that As(III) may be released only at strong alkali metals or high phosphate concentrations.

Ociński et al. [40] studied the As(III) and As(V) adsorption properties of the WTRs generated during the deironing and demanganization processes of infiltration water. Adsorption studies were carried out in a batch regime. As solutions were brought in contact with the GWTR powder in a 100 or 250 cm<sup>3</sup> conical flask. The effect of pH, initial concentration of As(III) and As(V), and time was evaluated. The maximum adsorption capacity determined by the Langmuir isotherm equations reached 132 mg/g for As(III) and 77 mg/g for As(V). The explanation of this trend is the oxidation of As(III) to As(V) accompanied with reductive dissolution of iron and manganese oxides. A significant factor for the sorption process is the presence of iron oxyhydroxides and humic substances in the residuals. The As(III) and As(V) removal efficiency was strongly dependent on the solution pH, with the best results obtained at pH 4.0, and a slight decrease in adsorption observed at pH 10.0. The removal of arsenic species was a rapid process and 90 min was required to remove 80% of the contaminant. Kinetic studies revealed two-step chemisorption of inner-sphere As(III) complexes. As(V) adsorption was controlled by external and intraparticle diffusion. Attempts were made to regenerate the GWTRs, but the values of desorption were low.

Ong et al. [89] evaluated the nickel ion adsorption capability of GWTRs. The effects of varying solution pH, initial nickel concentration, and contact time were investigated. The results showed that the pH (4.5 to 7.5) had no influence on Ni(II) removal. The maximum sorption capacity was 11.6 mg/g. The sorption isotherm was well-fitted to Freundlich equations. Sorption capacity increased with an increasing initial concentration. The equilibrium was achieved after 120 min. Sorption kinetic data was best-fitted to a pseudo-second-order adsorption kinetic model, indicating that chemisorption which is associated with the formation of a covalent bond through the exchange or sharing of electrons between metal ions and the binding sites of the adsorbent, was the dominant process [90].

We also conducted similar research, including batch sorption experiments of selected heavy metals and metalloids. The details concerning the methodology of the sorption experiments are in Section 2.2. The maximum amounts of removed Cr(III), Cr(VI), As(V), Cd(II), Pb(II), Zn(II), and Cu(II) were 22.3, 51.3, 24.8, 4.8, 92.7, 19.2, and 31.2 mg/g, respectively. The removal efficiency was strongly dependent on the initial metal concentration, which is a common trend in all presented researches. The sorption efficiency at the initial concentration of 100 mM/L was on average, 300 to 500 times higher than at a concentration of 0.1 mM/L. Cd(II) was the least adsorbed compound, while Pb(II) was the

best adsorbed. Due to the relatively high adsorption capacity of GWTRs toward all heavy metals and metalloids, the aim of further studies will be to measure the effect of pH, temperature, and time of reaction on sorption capacity.

## 5. Discussion

Table 4 shows the comparison of the specific surface area of all WTRs that are described in this paper, as well as their favorable adsorption test conditions. It is evident that sorption capacity depends on many different factors, such as the nature of sorbent surface, the properties of the sorbents, and the experimental conditions. WTRs create particles with irregular surfaces and edges, which provide WTRs with a highly reactive surface for sorption metals [52]. Sorption capacity also depends on the particle size of WTRs. The smaller particle size and therefore the higher surface area and the greater amounts of heavy metals and metalloids being sorbed. This trend was caused by an increasing surface area. Therefore, it is impossible to compare all these results, as the presented researches differ in sorption conditions and methodology.

As the results [4,40,61,68,87] showed, GWTRs exhibited better sorption capacity for As(III) and As(V) than SWTRs. The reason might be a higher concentration of iron and manganese oxides as well as a well-developed specific surface area [40,91]. However, in case of SWTRs, Al-SWTRs samples sorbed greater amounts of As(III) and As(V) than Fe-SWTRs. It might be explained by a higher surface area and higher organic matter content in Al-SWTRs. Fe-SWTRs was better sorbent in the case of As(III) than As(V), whereas more As(V) was sorbed by Al-SWTRs [4,87]. Se(IV), Se(VI), Cr(III), and Cr(VI) were removed in similar amounts. Among the cations, Hg(II) and Pb(II) were best sorbed, and Cd(II) and Ni(II) the least. However, the reason may be simply different sorption conditions. In most cases, sorption processes were dependent on pH and the best results were obtained for pH 6.0 to 7.0. Adsorption of the metal cations, (Pb(II), Cd(II), Co(II), and Ni(II)), on WTRs depends on pH, with an increasing pH of the solution the removal efficiency was higher [41,69,73,89]. It might be explained by the fact that metal ions form complexes with acidic functional groups in the sorbent [92]. In case of decreasing pH, protons compete with metal ions for the binding sites on the WTRs surface and the protons decrease the negative charges [73,79]. In case of anions, the lower pH favored the sorption capacity [3]. However, as Wu et al. [61] noted As(III) was favorably sorbed with pH 8.0. The further increase of the pH led to a decrease of As(III) removal and it could be attributed to the electrical repulsion force between GWTRs and As(III) anions. The most common sorption mechanism of metals and metalloids on WTRs was chemisorption, which involves an exchange between metal anions/cations and surface ligands and the formation of a covalent with the surface [85]. In most references, the sorption kinetic increased up to 120 min of experiments then decreased. Sorption of the described metals and metalloids was biphasic. The immediate sorption phase was followed by a much slower sorption phase. The rapid sorption might be due to the availability of active adsorption sites [3]. In almost all experiments, sorption capacity increased with an increase in the initial pollutant concentration. The sorption efficiency increased with increasing doses of adsorbent. This is assigned to the increasing surface area and number of adsorption sites with an increasing dose [69]. Temperatures were in the range of 23 to 25 °C, showing that the processes had been carried out at room temperature. However, sometimes the sorption process was more efficient in a higher temperature (20–50 °C), suggesting that sorption onto WTRs' surface is an endothermic process. This trend is noted for specifically adsorbing ions, which result in activation of the adsorbent surface [69,93]. Desorption has not been successful, only low values of contaminants were desorbed, and waste can be safely stored. For example, As(III) may be released only at strong alkali or high phosphate concentrations [61].

**Table 4.** Main characteristics and uptake capacities of WTRs for heavy metals and metalloids removal (SSA—specific surface area).

Adsorbent		Favorable Adsorption Test Conditions						Reference	
Type	SSA (m <sup>2</sup> /g)	Heavy Metals to be Removed	Initial Concentration (mg/L)	pH	Temp. (°C)	Contact Time (min)	Adsorption Capacity (mg/g)		
Fe-SWTRs	217.4	As(III)	80	7.0–9.0	-	24 h	11.2	[4]	
	-		200	-	23	60	14.5	[87]	
Fe-GWTRs	152		120	8.0	25	60	59.7	[61]	
	120		25	4.0	-	90	132.0	[40]	
Al-SWTRs	435.5		105	6.0–7.0	-	24 h	40.2	[4]	
	-		200	-	23	60	9.0	[87]	
	97.3		74	9.0	25	120	18.73	[68]	
Fe-SWTRs	217.4		As(V)	80	-	-	24 h	9.2	[4]
	-			200	-	23	60	10.0	[87]
Fe-GWTRs	120			25	4.0	-	90	77.0	[40]
	435.5			105	-	-	24 h	49.9	[4]
Al-SWTRs	-			200	-	23	60	15.0	[87]
	97.3	74		6.0	25	120	20.98	[68]	
	-	160		5.0–7.0	23	15	50.0	[3]	
	97.3	52		6.0–9.0	25	120	19.2	[69]	
	97.3	52		2.0–4.0	25	120	10.9		
	97.3	79		5.0	25	120	22.11	[68]	
	50	60		6.0–8.0	25	24 h	2.1	[73]	
	97.3	79		4.0	25	120	11.05	[68]	
	50	60	6.0–8.0	25	24 h	1.9	[73]		
	97.3	207	6.0–9.0	25	120	53.9	[69]		
-	40	3.0	-	32 h	79.0	[59]			
50	100	6.0–8.0	-	30	5.3	[73]			
Fe/Al-SWTRs	81.0	Co(II)	800	8.0	25	12 h	17.3	[41]	
GWTRs	-	Ni(II)	200	6.5	25	120	11.6	[89]	

## 6. Conclusions

The pollution of surface and groundwater with heavy metals is a major issue worldwide, and the development of suitable technology to remove heavy metals from the aqueous solutions is necessary. WTRs have a surprisingly good sorption capacity for different compounds, especially heavy metals and metalloids. The comparisons of sorption properties of various WTRs is difficult because of incoherence in the data, such as different chemical compositions of the treated water, various coagulants used, sorbent preparation, and testing methods. However, in most studies, the sorption efficiency was dependent on the pH of the solution, reaction time, temperature, and initial metal concentration in the solution. Decrease in particles size enhanced sorption properties due to increases in the specific surface area. The presence of iron and/or aluminum oxides was an important factor in the sorption process. WTRs are waste materials that can be used as low-cost, safe, and effective adsorbents for the removal of heavy metal cations and anions from polluted water. GWTRs, containing high iron and manganese oxides can be used to remove arsenic. As almost all of the publications presented above have proven, there are still many gaps in the knowledge about WTRs and their sorption properties. More research is required on the sorption mechanism, the desorption process as well as the long-term stability of formed metal–WTRs complexes. Sorption experiments of mixtures of selected compounds need to be carried out.

**Author Contributions:** T.B. designed and supervised the project; M.W. performed part of the experiments from this review, analyzed the data, and wrote this paper. T.B., M.K.-K., A.P., and G.R. submitted comments and corrected it.

**Funding:** This research was funded by the National Science Centre, Poland Grant No. 2017/27/N/ST10/00713 and PUT research project 01/13/DSPB/0891.

**Conflicts of Interest:** The authors declare no conflict of interest. The funders had no role in the design of the study; in the collection, analyses or interpretation of data; in the writing of the manuscript and in the decision to publish the results.

## References

1. Salem, H.M.; Eweida, E.A.; Farag, A. Heavy metals in drinking water and their environmental impact of human health. In Proceedings of the International Conference for Environmental Hazards Mitigation, Cairo, Egypt, 9–12 September 2000; pp. 542–556.
2. Burakov, A.E.; Galunin, E.V.; Burakova, I.V.; Kucherova, A.E.; Agarwal, S.; Tkachev, A.G.; Gupta, V.K. Adsorption of heavy metals on conventional and nanostructured materials for wastewater treatment purposes: A review. *Ecotoxicol. Environ. Saf.* **2018**, *148*, 702–712. [[CrossRef](#)] [[PubMed](#)]
3. Elkhatib, E.; Mahdy, A.; Sherif, F.; Hamadeen, H. Evaluation of a Novel Water Treatment Residual Nanoparticles as a Sorbent for Arsenic Removal. *J. Nanomater.* **2015**, *2015*, 10. [[CrossRef](#)]
4. Caporale, A.G.; Punamiya, P.; Pigna, M.; Violante, A.; Sarkar, D. Effect of particle size of drinking-water treatment residuals on the sorption of arsenic in the presence of competing ions. *J. Hazard. Mater.* **2013**, *260*, 644–651. [[CrossRef](#)] [[PubMed](#)]
5. Chen, Y.-Y.; Yu, S.-H.; Jiang, H.-F.; Yao, Q.-Z.; Fu, S.-Q.; Zhou, G.-T. Performance and mechanism of simultaneous removal of Cd(II) and Congo red from aqueous solution by hierarchical vaterite spherulites. *Appl. Surf. Sci.* **2018**, *444*, 224–234. [[CrossRef](#)]
6. Cao, W.; Wang, Z.; Ao, H.; Yuan, B. Removal of Cr(VI) by corn stalk based anion exchanger: The extent and rate of Cr(VI) reduction as side reaction. *Colloids Surf. A Physicochem. Eng. Asp.* **2018**, *539*, 424–432. [[CrossRef](#)]
7. Dinari, M.; Haghighi, A. Ultrasound-assisted synthesis of nanocomposites based on aromatic polyamide and modified ZnO nanoparticle for removal of toxic Cr(VI) from water. *Ultrason. Sonochem.* **2018**, *41*, 75–84. [[CrossRef](#)] [[PubMed](#)]
8. Lingamdinne, L.P.; Koduru, J.R.; Roh, H.; Choi, Y.-L.; Chang, Y.-Y.; Yang, J.-K. Adsorption removal of Co(II) from waste-water using graphene oxide. *Hydrometallurgy* **2016**, *165*, 90–96. [[CrossRef](#)]
9. Hu, H.M.; Li, X.W.; Huang, P.W.; Zhang, Q.W.; Yuan, W.Y. Efficient removal of copper from wastewater by using mechanically activated calcium carbonate. *J. Environ. Manag.* **2017**, *203*, 1–7. [[CrossRef](#)] [[PubMed](#)]

10. Khatri, N.; Tyagi, S.; Rawtani, D. Recent strategies for the removal of iron from water: A review. *J. Water Process. Eng.* **2017**, *19*, 291–304. [[CrossRef](#)]
11. Liu, J.; Mwamulima, T.; Wang, Y.; Fang, Y.; Song, S.; Peng, C. Removal of Pb(II) and Cr(VI) from aqueous solutions using the fly ash-based adsorbent material-supported zero-valent iron. *J. Mol. Liq.* **2017**, *243*, 205–211. [[CrossRef](#)]
12. Dubey, R.; Bajpai, J.; Bajpai, A. Chitosan-alginate nanoparticles (CANPs) as potential nanosorbent for removal of Hg (II) ions. *Environ. Nanotechnol. Monit. Manag.* **2016**, *6*, 32–44. [[CrossRef](#)]
13. Ali, I. The Quest for Active Carbon Adsorbent Substitutes: Inexpensive Adsorbents for Toxic Metal Ions Removal from Wastewater. *Sep. Purif. Rev.* **2010**, *39*, 95–171. [[CrossRef](#)]
14. Zhang, X.T.; Wang, X.M. Adsorption and Desorption of Nickel(II) Ions from Aqueous Solution by a Lignocellulose/Montmorillonite Nanocomposite. *PLoS ONE* **2015**, *10*, e0117077. [[CrossRef](#)]
15. Hoseinian, F.S.; Rezai, B.; Kowsari, E.; Safari, M. Kinetic study of Ni(II) removal using ion flotation: Effect of chemical interactions. *Miner. Eng.* **2018**, *119*, 212–221. [[CrossRef](#)]
16. Omraei, M.; Esfandian, H.; Katal, R.; Ghorbani, M. Study of the removal of Zn(II) from aqueous solution using polypyrrole nanocomposite. *Desalination* **2011**, *271*, 248–256. [[CrossRef](#)]
17. Fu, F.; Wang, Q. Removal of heavy metal ions from wastewaters: A review. *J. Environ. Manag.* **2011**, *92*, 407–418. [[CrossRef](#)]
18. Mauchauffée, S.; Meux, E. Use of sodium decanoate for selective precipitation of metals contained in industrial wastewater. *Chemosphere* **2007**, *69*, 763–768. [[CrossRef](#)]
19. Verma, V.; Tewari, S.; Rai, J. Ion exchange during heavy metal bio-sorption from aqueous solution by dried biomass of macrophytes. *Bioresour. Technol.* **2008**, *99*, 1932–1938. [[CrossRef](#)]
20. Lai, Y.-C.; Chang, Y.-R.; Chen, M.-L.; Lo, Y.-K.; Lai, J.-Y.; Lee, D.-J. Poly(vinyl alcohol) and alginate cross-linked matrix with immobilized Prussian blue and ion exchange resin for cesium removal from waters. *Bioresour. Technol.* **2016**, *214*, 192–198. [[CrossRef](#)]
21. Cochrane, E.; Lu, S.; Gibb, S.; Villaescusa, I.; Gibb, S. A comparison of low-cost biosorbents and commercial sorbents for the removal of copper from aqueous media. *J. Hazard. Mater.* **2006**, *137*, 198–206. [[CrossRef](#)]
22. Davarnejad, R.; Panahi, P. Cu (II) removal from aqueous wastewaters by adsorption on the modified Henna with Fe<sub>3</sub>O<sub>4</sub> nanoparticles using response surface methodology. *Sep. Purif. Technol.* **2016**, *158*, 286–292. [[CrossRef](#)]
23. Landaburu-Aguirre, J.; Pongracz, E.; Peramaki, P.; Keiski, R.L. Micellar-enhanced ultrafiltration for the removal of cadmium and zinc: Use of response surface methodology to improve understanding of process performance and optimisation. *J. Hazard. Mater.* **2010**, *180*, 524–534. [[CrossRef](#)]
24. Rahmanian, B.; Pakizeh, M.; Esfandyari, M.; Heshmatnezhad, F.; Maskooki, A. Fuzzy modeling and simulation for lead removal using micellar-enhanced ultrafiltration (MEUF). *J. Hazard. Mater.* **2011**, *192*, 585–592. [[CrossRef](#)]
25. Mohsen-Nia, M.; Montazeri, P.; Modarress, H. Removal of Cu<sup>2+</sup> and Ni<sup>2+</sup> from wastewater with a chelating agent and reverse osmosis processes. *Desalination* **2007**, *217*, 276–281. [[CrossRef](#)]
26. Yoon, J.; Amy, G.; Chung, J.; Sohn, J.; Yoon, Y. Removal of toxic ions (chromate, arsenate, and perchlorate) using reverse osmosis, nanofiltration, and ultrafiltration membranes. *Chemosphere* **2009**, *77*, 228–235. [[CrossRef](#)]
27. Lertlapwasin, R.; Bhawawet, N.; Imyim, A.; Fuangswasdi, S. Ionic liquid extraction of heavy metal ions by 2-aminothiophenol in 1-butyl-3-methylimidazolium hexafluorophosphate and their association constants. *Sep. Purif. Technol.* **2010**, *72*, 70–76. [[CrossRef](#)]
28. Akbal, F.; Camci, S. Copper, chromium and nickel removal from metal plating wastewater by electrocoagulation. *Desalination* **2011**, *269*, 214–222. [[CrossRef](#)]
29. Dharnaik, A.S.; Ghosh, P.K. Hexavalent chromium Cr(VI) removal by the electrochemical ion-exchange process. *Environ. Technol.* **2014**, *35*, 2272–2279. [[CrossRef](#)]
30. Lee, C.G.; Jeon, J.W.; Hwang, M.J.; Ahn, K.H.; Park, C.; Choi, J.W.; Lee, S.H. Lead and copper removal from aqueous solutions using carbon foam derived from phenol resin. *Chemosphere* **2015**, *130*, 59–65. [[CrossRef](#)]
31. Maneechakr, P.; Karnjanakom, S. Adsorption behaviour of Fe(II) and Cr(VI) on activated carbon: Surface chemistry, isotherm, kinetic and thermodynamic studies. *J. Chem. Thermodyn.* **2017**, *106*, 104–112. [[CrossRef](#)]
32. Petrus, R.; Warchol, J.K. Heavy metal removal by clinoptilolite. An equilibrium study in multi-component systems. *Water Res.* **2005**, *39*, 819–830. [[CrossRef](#)]

33. Bajda, T.; Kłapyta, Z. Adsorption of chromate from aqueous solutions by HDTMA-modified clinoptilolite, glauconite and montmorillonite. *Appl. Clay Sci.* **2013**, *86*, 169–173. [[CrossRef](#)]
34. Bajda, T.; Szala, B.; Solecka, U. Removal of lead and phosphate ions from aqueous solutions by organo-smectite. *Environ. Technol.* **2015**, *36*, 2872–2883. [[CrossRef](#)]
35. He, Y.; Liu, Q.Q.; Hu, J.; Zhao, C.X.; Peng, C.J.; Yang, Q.; Wang, H.L.; Liu, H.L. Efficient removal of Pb(II) by amine functionalized porous organic polymer through post-synthetic modification. *Sep. Purif. Technol.* **2017**, *180*, 142–148. [[CrossRef](#)]
36. Wang, Y.Y.; Liu, Y.X.; Lu, H.H.; Yang, R.Q.; Yang, S.M. Competitive adsorption of Pb(II), Cu(II), and Zn(II) ions onto hydroxyapatite-biochar nanocomposite in aqueous solutions. *J. Solid State Chem.* **2018**, *261*, 53–61. [[CrossRef](#)]
37. Chen, J.G.; Kong, H.N.; Wu, D.Y.; Chen, X.C.; Zhang, D.L.; Sun, Z.H. Phosphate immobilization from aqueous solution by fly ashes in relation to their composition. *J. Hazard. Mater.* **2007**, *139*, 293–300. [[CrossRef](#)]
38. Lim, J.W.; Chang, Y.Y.; Yang, J.K.; Lee, S.M. Adsorption of arsenic on the reused sanding wastes calcined at different temperatures. *Colloids Surf. A Physicochem. Eng. Asp.* **2009**, *345*, 65–70. [[CrossRef](#)]
39. Lingamdinne, L.P.; Yang, J.K.; Chang, Y.Y.; Koduru, J.R. Low-cost magnetized *Lonicera japonica* flower biomass for the sorption removal of heavy metals. *Hydrometallurgy* **2016**, *165*, 81–89. [[CrossRef](#)]
40. Ocinski, D.; Jacukowicz-Sobala, I.; Mazur, P.; Raczyk, J.; Kociolek-Balawejder, E. Water treatment residuals containing iron and manganese oxides for arsenic removal from water—Characterization of physicochemical properties and adsorption studies. *Chem. Eng. J.* **2016**, *294*, 210–221. [[CrossRef](#)]
41. Jiao, J.; Zhao, J.B.; Pei, Y.S. Adsorption of Co(II) from aqueous solutions by water treatment residuals. *J. Environ. Sci.* **2017**, *52*, 232–239. [[CrossRef](#)]
42. Rzepa, G.; Bajda, T.; Ratajczak, T. Utilization of bog iron ores as sorbents of heavy metals. *J. Hazard. Mater.* **2009**, *162*, 1007–1013. [[CrossRef](#)]
43. Jia, Y.F.; Demopoulos, G.P. Adsorption of arsenate onto ferrihydrite from aqueous solution: Influence of media (sulfate vs nitrate), added gypsum, and pH alteration. *Environ. Sci. Technol.* **2005**, *39*, 9523–9527. [[CrossRef](#)]
44. Gao, Y.; Mucci, A. Individual and competitive adsorption of phosphate and arsenate on goethite in artificial seawater. *Chem. Geol.* **2003**, *199*, 91–109. [[CrossRef](#)]
45. Violante, A.; Pucci, M.; Cozzolino, V.; Zhu, J.; Pigna, M. Sorption/desorption of arsenate on/from Mg-Al layered double hydroxides: Influence of phosphate. *J. Colloid Interface Sci.* **2009**, *333*, 63–70. [[CrossRef](#)]
46. Xie, J.K.; Xu, H.M.; Qu, Z.; Huang, W.J.; Chen, W.M.; Ma, Y.P.; Zhao, S.J.; Liu, P.; Yan, N.Q. Sn-Mn binary metal oxides as non-carbon sorbent for mercury removal in a wide-temperature window. *J. Colloid Interface Sci.* **2014**, *428*, 121–127. [[CrossRef](#)]
47. Zhang, W.; Liu, C.H.; Zheng, T.; Ma, J.; Zhang, G.S.; Ren, G.H.; Wang, L.; Liu, Y.L. Efficient oxidation and sorption of arsenite using a novel titanium (IV)-manganese(IV) binary oxide sorbent. *J. Hazard. Mater.* **2018**, *353*, 410–420. [[CrossRef](#)]
48. Mikhaylov, V.I.; Maslennikova, T.P.; Krivoschapkina, E.F.; Tropnikov, E.M.; Krivoschapkin, P.V. Express Al/Fe oxide-oxyhydroxide sorbent systems for Cr(VI) removal from aqueous solutions. *Chem. Eng. J.* **2018**, *350*, 344–355. [[CrossRef](#)]
49. Altundogan, H.S.; Altundogan, S.; Tumen, F.; Bildik, M. Arsenic adsorption from aqueous solutions by activated red mud. *Waste Manag.* **2002**, *22*, 357–363. [[CrossRef](#)]
50. Evuti, A.M.; Lawal, M. Recovery of coagulants from water works sludge: A review. *Adv. Appl. Sci. Res.* **2011**, *2*, 410–417.
51. Magdalena, W.; Tomasz, B. Current stage of knowledge relating to the use of ferruginous sludge from water treatment plants—A preliminary review of the literature. *Mineralogia* **2017**, *48*, 9–45.
52. Quinones, K.D.; Hovsepyan, A.; Oppong-Anane, A.; Bonzongo, J.C.J. Insights into the mechanisms of mercury sorption onto aluminum based drinking water treatment residuals. *J. Hazard. Mater.* **2016**, *307*, 184–192. [[CrossRef](#)]
53. Wołowiec, M.; Pruss, A.; Komorowska-Kaufman, M.; Lasocka-Gomuła, I.; Rzepa, G.; Bajda, T. The properties of sludge formed as a result of coagulation of backwash water from filters removing iron and manganese from groundwater. *SN Appl. Sci.* **2019**, *1*, 639. [[CrossRef](#)]

54. Komorowska-Kaufman, M. Adsorption properties of sludge arising during processes of groundwater and surface water treatment—A review. In *Sorbenty Mineralne—Surowce, Energetyka, Ochrona Środowiska, Nowoczesne Technologie*; Bajda, T., Ed.; Wydawnictwo Naukowe AGH: Kraków, Polska, 2017; pp. 65–75.
55. Babatunde, A.O.; Zhao, Y.Q. Constructive approaches toward water treatment works sludge management: An international review of beneficial reuses. *Crit. Rev. Environ. Sci. Technol.* **2007**, *37*, 129–164. [[CrossRef](#)]
56. Yang, L.; Wei, J.; Zhang, Y.M.; Wang, J.L.; Wang, D.T. Reuse of acid coagulant-recovered drinking waterworks sludge residual to remove phosphorus from wastewater. *Appl. Surf. Sci.* **2014**, *305*, 337–346. [[CrossRef](#)]
57. Krishna, K.C.B.; Aryal, A.; Jansen, T. Comparative study of ground water treatment plants sludges to remove phosphorous from wastewater. *J. Environ. Manag.* **2016**, *180*, 17–23. [[CrossRef](#)]
58. Makris, K.C.; Harris, W.G.; O'Connor, G.A.; Obreza, T.A. Phosphorus immobilization in micropores of drinking-water treatment residuals: Implications for long-term stability. *Environ. Sci. Technol.* **2004**, *38*, 6590–6596. [[CrossRef](#)]
59. Hovsepyan, A.; Bonzongo, J.C.J. Aluminum drinking water treatment residuals (Al-WTRs) as sorbent for mercury: Implications for soil remediation. *J. Hazard. Mater.* **2009**, *164*, 73–80. [[CrossRef](#)]
60. Gibbons, M.K.; Gagnon, G.A. Understanding removal of phosphate or arsenate onto water treatment residual solids. *J. Hazard. Mater.* **2011**, *186*, 1916–1923. [[CrossRef](#)]
61. Wu, K.; Liu, R.P.; Li, T.; Liu, H.J.; Peng, J.M.; Qu, J.H. Removal of arsenic(III) from aqueous solution using a low-cost by-product in Fe-removal plants-Fe-based backwashing sludge. *Chem. Eng. J.* **2013**, *226*, 393–401. [[CrossRef](#)]
62. Sales, A.; de Souza, F.R.; Almeida, F.D.R. Mechanical properties of concrete produced with a composite of water treatment sludge and sawdust. *Constr. Build. Mater.* **2011**, *25*, 2793–2798. [[CrossRef](#)]
63. Ahmad, T.; Ahmad, K.; Ahad, A.; Alam, M. Characterization of water treatment sludge and its reuse as coagulant. *J. Environ. Manag.* **2016**, *182*, 606–611. [[CrossRef](#)]
64. Vinitnantharat, S.; Kositchaiyong, S.; Chiarakorn, S. Removal of fluoride in aqueous solution by adsorption on acid activated water treatment sludge. *Appl. Surf. Sci.* **2010**, *256*, 5458–5462. [[CrossRef](#)]
65. Yang, Y.; Tomlinson, D.; Kennedy, S.; Zhao, Y.Q. Dewatered alum sludge: A potential adsorbent for phosphorus removal. *Water Sci. Technol.* **2006**, *54*, 207–213. [[CrossRef](#)]
66. Kyncl, M.; Číhalová, Š.; Juroková, M.; Langarová, S. Disposal and reuse of the water processing sludge. *Inž. Miner.* **2012**, *2*, 11–20.
67. Szerzyna, S. *Porcjowe Grawitacyjne Zagęszczenie Osadów Powstających W Różnych Układach Oczyszczania Wody*; Politechnika Wroclawska: Wrocław, Polska, 2012.
68. Zhou, Y.F.; Haynes, R.J. A Comparison of Water Treatment Sludge and Red Mud as Adsorbents of As and Se in Aqueous Solution and Their Capacity for Desorption and Regeneration. *Water Air Soil Pollut.* **2012**, *223*, 5563–5573. [[CrossRef](#)]
69. Zhou, Y.F.; Haynes, R.J. Removal of Pb(II), Cr(III) and Cr(VI) from Aqueous Solutions Using Alum-Derived Water Treatment Sludge. *Water Air Soil Pollut.* **2011**, *215*, 631–643. [[CrossRef](#)]
70. Wang, C.H.; Yuan, N.N.; Pei, Y.S. Effect of pH on Metal Lability in Drinking Water Treatment Residuals. *J. Environ. Qual.* **2014**, *43*, 389–397. [[CrossRef](#)]
71. USEPA. *The Toxicity Characteristic Leaching Procedure*; USEPA: Washington, DC, USA, 1992.
72. Ippolito, J.A.; Scheckel, K.G.; Barbarick, K.A. Selenium adsorption to aluminum-based water treatment residuals. *J. Colloid Interface Sci.* **2009**, *338*, 48–55. [[CrossRef](#)]
73. Siswoyo, E.; Mihara, Y.; Tanaka, S. Determination of key components and adsorption capacity of a low cost adsorbent based on sludge of drinking water treatment plant to adsorb cadmium ion in water. *Appl. Clay Sci.* **2014**, *97–98*, 146–152. [[CrossRef](#)]
74. Postawa, A. *Best Practice Guide on the Control of Iron and Manganese in Water Supply*; Hayes, C., Ed.; IWA Publishing: London, UK, 2013; p. 131.
75. Pruss, A.; Jeż-Walkowiak, J.; Sozański, M.M. Concentration of heavy metals on surface of filter materials and in backwash water. In *Metals and Related Substances in Drinking Water, COST Action 637, Proceedings of the 4th International Conference of METEAU, Kristianstad, Sweden, 13–15 October 2010*; IWA Publishing: London, UK, 2011; pp. 217–222.

76. Jez-Walkowiak, J.; Pruss, A.; Sozański, M.M. Applied technologies and possibilities of modernization of groundwater treatment plants in Poland. In *Metals and Related Substances in Drinking Water, COST Action 637, Proceedings of the 4th International Conference of METEAU, Kristianstad, Sweden, 13–15 October 2010*; IWA Publishing: London, UK, 2011; pp. 172–175.
77. Pruss, A.; Pruss, P.; Jedrzejczak, A. Hydraulic losses generated by modern drainage systems during backwash of rapid filters. *Ochr. Śr.* **2011**, *33*, 47–48.
78. Dixit, S.; Hering, J.G. Comparison of arsenic(V) and arsenic(III) sorption onto iron oxide minerals: Implications for arsenic mobility. *Environ. Sci. Technol.* **2003**, *37*, 4182–4189. [[CrossRef](#)]
79. Kadirvelu, K.; Namasivayam, C. Activated carbon from coconut coirpith as metal adsorbent: Adsorption of Cd(II) from aqueous solution. *Adv. Environ. Res.* **2004**, *8*, 729. [[CrossRef](#)]
80. Rao, M.M.; Ramesh, A.; Rao, G.P.C.; Seshaiyah, K. Removal of copper and cadmium from the aqueous solutions by activated carbon derived from Ceiba pentandra hulls. *J. Hazard. Mater.* **2006**, *129*, 123–129. [[CrossRef](#)]
81. Wang, Y.; Tang, X.W.; Chen, Y.M.; Zhan, L.T.; Li, Z.Z.; Tang, Q. Adsorption behavior and mechanism of Cd(II) on loess soil from China. *J. Hazard. Mater.* **2009**, *172*, 30–37. [[CrossRef](#)]
82. Gupta, V.K.; Jain, C.K.; Ali, I.; Sharma, M.; Saini, V.K. Removal of cadmium and nickel from wastewater using bagasse fly ash—A sugar industry waste. *Water Res.* **2003**, *37*, 4038–4044. [[CrossRef](#)]
83. Axe, L.; Trivedi, P. Intraparticle surface diffusion of metal contaminants and their attenuation in microporous amorphous Al, Fe, and Mn oxides. *J. Colloid Interface Sci.* **2002**, *247*, 259–265. [[CrossRef](#)]
84. Wang, C.H.; Guo, W.; Tian, B.H.; Pei, Y.S.; Zhang, K.J. Characteristics and kinetics of phosphate adsorption on dewatered ferric-alum residuals. *J. Environ. Sci. Health Part A Toxic/Hazard. Subst. Environ. Eng.* **2011**, *46*, 1632–1639. [[CrossRef](#)]
85. McBride, M.B. Chemisorption and precipitation reactions. In *Handbook of Soil Science*; Sumner, M.E., Ed.; CRC Press: Boca Raton, FL, USA, 2000; pp. 265–302.
86. Ho, Y.S.; McKay, G. Pseudo-second order model for sorption processes. *Process. Biochem.* **1999**, *34*, 451–465. [[CrossRef](#)]
87. Makris, K.C.; Sarkar, D.; Datta, R. Evaluating a drinking-water waste by-product as a novel sorbent for arsenic. *Chemosphere* **2006**, *64*, 730–741. [[CrossRef](#)]
88. Stumm, W. *Chemistry of the Solid-Water Interface*; John Wiley & Sons, Inc.: Chichester, UK, 1992.
89. Ong, D.C.; Kan, C.C.; Pingul-Ong, S.M.B.; de Luna, M.D.G. Utilization of groundwater treatment plant (GWTP) sludge for nickel removal from aqueous solutions: Isotherm and kinetic studies. *J. Environ. Chem. Eng.* **2017**, *5*, 5746–5753. [[CrossRef](#)]
90. de Luna, M.D.G.; Flores, E.D.; Genuino, D.A.D.; Futralan, C.M.; Wan, M.W. Adsorption of Eriochrome Black T (EBT) dye using activated carbon prepared from waste rice hulls—Optimization, isotherm and kinetic studies. *J. Taiwan Inst. Chem. Eng.* **2013**, *44*, 646–653. [[CrossRef](#)]
91. Oliveira, L.C.A.; Rios, R.; Fabris, J.D.; Sapag, K.; Garg, V.K.; Lago, R.M. Clay-iron oxide magnetic composites for the adsorption of contaminants in water. *Appl. Clay Sci.* **2003**, *22*, 169–177. [[CrossRef](#)]
92. Khalfa, L.; Bagane, M. Cadmium removal from aqueous solution by a Tunisian smectitic natural and activated clay: Thermodynamic study. *J. Encapsul. Adsorpt. Sci.* **2011**, *1*, 65–71. [[CrossRef](#)]
93. Ramesh, A.; Hasegawa, H.; Maki, T.; Ueda, K. Adsorption of inorganic and organic arsenic from aqueous solutions by polymeric Al/Fe modified montmorillonite. *Sep. Purif. Technol.* **2007**, *56*, 90–100. [[CrossRef](#)]

